Kinetics of excited muonic hydrogen

Wilhelm Czapliński and Adam Guła
Faculty of Physics and Nuclear Techniques, University of Mining and Metallurgy, al. Mickiewicza 30, PL-30-059 Cracow, Poland

Andrei Kravtsov and Alexander Mikhailov
Petersburg Nuclear Physics Institute, 188350 Gatchina, Russian Federation

Nicolai Popov
Sektion Physik der Universität München, Schellingstrasse 4, 80799 München, Germany
(Received 22 October 1993; revised manuscript received 7 March 1994)

Deexcitation and charge exchange of excited muonic hydrogen are considered. The inverse quasiresonant charge exchange process is taken into account. During cascade the inverse charge exchange balances the direct process down to the level with the principal quantum number $\bar{n}$ for which the resonance defect is larger than the collision energy. The density of the muonic atom for $n \leq \bar{n}$ is then determined by deexcitation and muon transfer to nuclei of heavier hydrogen isotopes. Energy dependence of the ground-state population of the initial muonic hydrogen, q_{1s}, is considered. Comparing our results for the q_{1s} parameter with the available experimental data, we conclude that the collision energy of the excited muonic atoms is ~ 3 eV for D-T and ~ 5 eV for an H-D mixture.

PACS number(s): 34.60.+z, 36.10.Gv, 34.70.+e, 82.30.Fi

I. INTRODUCTION

The slowing down and atomic capture of negative muons by hydrogen have been investigated theoretically in Refs. [1–6]. These processes present the first stage of the formation of muonic hydrogen atoms and determine their initial energy distribution in gaseous or liquid targets. Since there are no direct corresponding experimental data, the theoretical predictions become very important.

Different theoretical approaches have been used to describe inelastic muon collisions with hydrogen atoms [2–4] and molecules [6]. The pioneering quasiclassical treatment [1] with the approximation of the stopping medium as an electron gas is more adequate for muon collisions with multielectron atoms. Since the average muon energy varies from a few eV to several keV, different methods are adequate for various muon energies. Side by side with Born approximation for high-energy muons, other quantum-mechanical and classical calculations were adopted for low-to-intermediate energies, in particular, the diabatic-state treatment of muon capture [2], as well as the classical-trajectory Monte Carlo method [3]. The model of inelastic collisions of muons with hydrogen molecules in the framework of the adiabatic representation method by the system of coupled-channel equations was considered in Refs. [6].

After formation of muonic hydrogen in the mixture of hydrogen isotopes its destiny is determined by deexcitation and muon transfer to heavier nuclei. Such processes were considered, e.g., in Ref. [7]. As for muon transfer processes, in contrast with previous publications, we take into account in the present paper also the inverse muon transfer (from heavier to lighter nucleus of hydrogen isotope) for collision energies ε exceeding the resonance defect for a given principal quantum number n. As a result we can explain the experimental data on the ground-state population q_{1s} of muonic deuterium in D-T mixture [8], considering the kinetics of the excited muonic atoms at collision energies $2 < \varepsilon \leq 3$ eV. The available experimental data for H-D mixture [9] can be explained assuming collision energy ranges between 5 and 6 eV (see Sec. IV).

II. DEEXCITATION PROCESSES

Radiative and external Auger deexcitation modes of the excited muonic hydrogen as well as deexcitation via target molecule dissociation and Coulomb deexcitation were considered by Leon and Bethe [10]. Auger deexcitation was considered in the Born [10] and eikonal [11] approximation. For transitions shown in Fig. 1, we used the rates of radiative deexcitation from Ref. [12] (see Table I).

The decisive role in the deexcitation of the muonic hydrogen immediately after Coulomb muon capture belongs probably to the chemical reactions involving the dissociation of the target molecules (dissociation energy for hydrogen molecule is $\varepsilon_{dis} \sim 4.7$ eV). In the present paper,

TABLE I. Radiative deexcitation rates of muonic atom (see Ref. [12]).

$(n,l)_i \rightarrow (n,l)_f$	$\lambda_{rad}(10^{10}\ s^{-1})$
$2p \rightarrow 1s$	13
$3s \rightarrow 2p$	0.12
$3p \rightarrow 2s$	0.43
$3p \rightarrow 1s$	3.5
$3d \rightarrow 2p$	1.3
$4 \rightarrow 1s$	0.3

 ©1994 The American Physical Society

TABLE II. Rates for $d\mu$ deexcitation caused by molecule dissociation calculated according to Ref. [10] for collision energy $\varepsilon = 1$ eV.

$n_i \rightarrow n_f$	$\lambda_{mol}(10^{10}\ s^{-1})$
$8 \rightarrow 7$	12
$9 \rightarrow 8$	19
$10 \rightarrow 9$	29
$11 \rightarrow 9$	42
$12 \rightarrow 10$	59

molecular dissociation is considered for excited muonic atom states with the principal quantum numbers $8 \leq n \leq 12$ (see Fig. 1). Following Ref. [10] the corresponding cross sections are approximated by the geometrical ones (the transition rates are then proportional to $\sqrt{\varepsilon}$) which seems to be justified for collision energy $\varepsilon < \varepsilon_{dis}$ only. On the other hand, as it was shown in Sec. III of the paper, the q_{1s} parameter practically does not depend on deexcitation processes for the states $n > 4$ at collision energy $\varepsilon > 2$ eV for D-T, and $n > 6$, at $\varepsilon = 5$ eV for the H-D mixture. Therefore, the energy dependence of cross section for $\varepsilon > \varepsilon_{dis}$ is rather unimportant for our q_{1s} results. The rates of deexcitation caused by molecule dissociation, calculated for collision energy $\varepsilon = 1.0$ eV according to Ref. [10], are presented in Table II.

Auger deexcitation rates were calculated for muonic hydrogen using the values obtained for pionic hydrogen in Ref. [10] (see Table III). As for the Stark mixing of $2p$ and $2s$ states and the induced $2s \rightarrow 2p \rightarrow 1s$ transition, we follow the results of Refs. [13–18]. For collision energy larger than the $2p$-$2s$ Lamb shift, i.e., $\varepsilon > 0.2$ eV, the directs $2s \rightarrow 2p$ transition is energetically allowed and its rate exceeds $\lambda_{ind}(2s \rightarrow 2p \rightarrow 1s)$. The rates of $2s \rightarrow 2p$, $2p \rightarrow 2s$, and λ_{ind} are given in Table IV.

The process of Coulomb deexcitation, which was mentioned in Ref. [10],

$$(H\mu)^*_n + H' \rightarrow (H\mu)^*_{n-1} + H' \qquad (1)$$

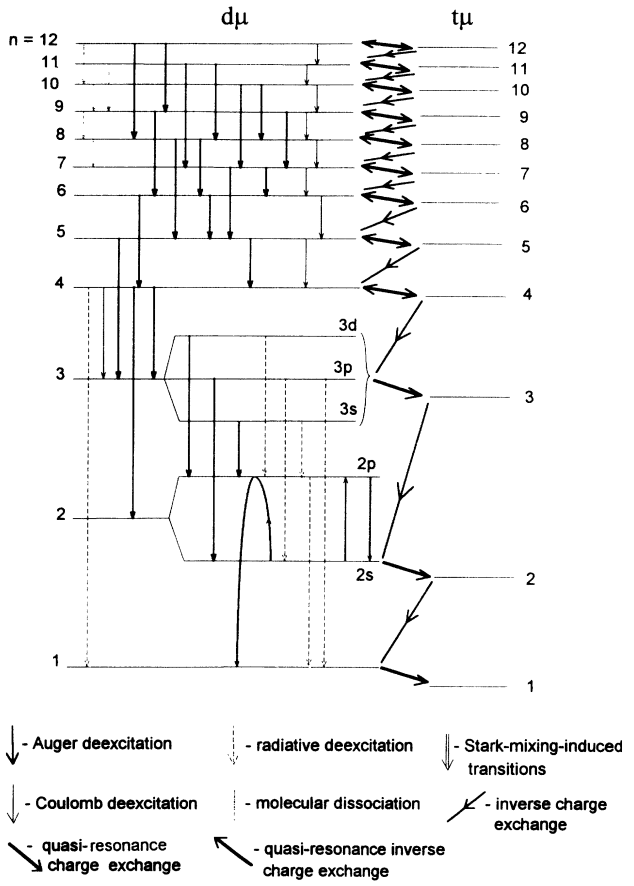

FIG. 1. Scheme of $d\mu$ atom deexcitation and muon transfer processes in the collisions with tritium.

$(H,H' = p,d,t$ and $n \geq 2)$ requires a special consideration. The numerical analysis of reaction (1) for symmetric case $H = H'$ was performed in Refs. [19–22].

We use the quasiclassical approximation, which is justified for the interaction of the excited muonic hydro-

TABLE III. Auger deexcitation rates for $d\mu$ atom ($10^{10}\ s^{-1}$) were calculated using the rates of pionic hydrogen [10]. The rate for the $12 \rightarrow 9$ transition is allowed for the collision of the $d\mu$ atom with the hydrogen isotope atom only (not the molecule).

n_i \ n_f	2s	2	2p	3	4	5	6	7	8	9
3s			1.8							
3p	6.4									
3d			18							
4		0.8		97						
5				6.3	428					
6					28	1372				
7						89	3393			
8						16	251			
9							43	457		
10								91	900	
11								28	177	
12									56	310

TABLE IV. Rates for $2s \rightarrow 2p$, $2p \rightarrow 2s$, and $2s \rightarrow 2p \rightarrow 1s$ transitions in the $d\mu$ atom.

Collision energy (eV)	$d\mu$+D collisions λ (10^{10} s^{-1}) $2p \rightarrow 2s$	$d\mu$+D collisions λ (10^{10} s^{-1}) $2s \rightarrow 2p$	$d\mu$+T collisions λ (10^{10} s^{-1}) $2p \rightarrow 2s$	$d\mu$+T collisions λ (10^{10} s^{-1}) $2s \rightarrow 2p$	2s-2p-1s transition λ_{ind} (10^{10} s^{-1})
0.01	0.00	0.00	0.01	0.00	0.25
0.02	0.01	0.00	0.04	0.00	0.32
0.04	0.04	0.00	0.16	0.00	0.40
0.06	0.10	0.00	0.33	0.00	0.42
0.08	0.21	0.00	0.61	0.00	0.45
0.10	0.36	0.00	0.91	0.00	0.47
0.50	100.10	300.31	100.10	300.31	9.80
1.00	157.30	471.90	157.30	471.90	9.80
2.00	222.45	667.36	222.45	667.36	9.80
3.00	272.45	817.35	272.45	817.35	9.80
4.00	314.60	943.79	314.60	943.79	9.80
5.00	351.73	1055.19	351.73	1055.19	9.80

gen with nuclei according to the validity condition $d\lambda/dR \ll 1$, where λ is the wavelength of the muonic atom and R is the internuclear distance. Thus one may consider that the muonic atom moves along a classical trajectory with an impact parameter ρ.

In the framework of this approximation the cross section is given by

$$\sigma = \pi \int_0^{\rho_{\max}^2} P \, d\rho^2 , \tag{2}$$

where P is the reaction probability

$$P = 2\exp(-2\delta)[1-\exp(-2\delta)] \tag{3}$$

with Massey parameter

$$\delta = \left| \mathrm{Im} \int_C p(R) dR \right| , \tag{4}$$

where $p(R) = Mv\sqrt{1-U/\varepsilon-(\rho/R)^2}$ is the radial momentum, M is the reduced mass of colliding atoms, v is the relative velocity of colliding particles at $R \rightarrow \infty$, $\varepsilon = Mv^2/2$ is the collision energy. The effective potential U of the interaction of an excited muonic hydrogen, having parabolic quantum numbers (n,n_1,n_2,m), with a hydrogen nucleus corresponds to the molecular term of the two center Coulomb problem which is asymptotically determined by linear Stark effect.

The molecular terms corresponding to the initial and final states of reaction (1) and their crossing points are evaluated in the complex plane of the internuclear distance R [23]. According to the theory, the transition probability is completely determined by the analytic properties of terms, corresponding to the initial and final states of the system, being large mainly in the region of quasicrossing of the terms in question, i.e., in the region close to the singularities (branch points) of the terms. The transition region is passed twice in accordance with Eq. (3).

The integral in Eq. (4) is taken along a contour C enclosing the branch point R_c in the complex R plane. The maximum impact parameter $\rho_{\max}$ in Eq. (2) is determined by the requirement that $p(R)$ be real at the trajectory, i.e., for $R \geq \mathrm{Re}R_c$.

According to Ref. [23] the branch points responsible for reaction (1) belong to the T series, which connects the terms with parabolic quantum numbers (n,n_1,n_2,m) and $(n-1,n_1,n_2-1,m)$.

If $H = H'$, one should distinguish symmetric (gerade) g states and antisymmetric (ungerade) u states. Both g and u states have a common T series of branch points with the same $\mathrm{Re}R_t$, but $\mathrm{Im}R_{tu} \simeq 2\mathrm{Im}R_{tg}$. For this reason, due to large values of Massey parameters, the transition between the u terms has a much lower probability (with the possible exception of a very large n, where the Massey parameters are small due to small ΔU values). Coordinates of the T series of branch points were calculated approximately with the help of the semiclassical approximation for the terms calculated in Ref. [24(a)]. Table V contains our branch points calculated numerically for symmetric (gerade) terms for $n \geq 4$.

In contrast with Refs. [21 and 22], the exact values of terms, calculated in semiclassical approximation [24a], are used in the present paper to obtain Massey parameters.

Only attractive initial states (with $n_1 < n_2$) that give the largest contribution to cross section due to the "focusing" of the particles were considered. The screening of the charge of the hydrogen nucleus by atomic electrons was taken into account in the same manner as in Ref. [7].

The cross section of reaction (1) is

$$\sigma_n = \sum_{\Delta<0} [(n-|\Delta|)/n^2]\sigma_n(\Delta) , \tag{5}$$

where $\Delta = n_1 - n_2$. If $H = H'$, $\sigma_n(\Delta)$ is an average over the g and u states and

$$\sigma_n = \sum_m [(2-\delta_{0m})/n^2](1/2)[\sigma_g(n,m)+\sigma_u(n,m)] , \tag{6}$$

where $\sigma_{g,u}$ is the cross section corresponding to the symmetric or antisymmetric state.

If mass M_1 of the nucleus H is smaller than that of H', M_2, the initial term becomes an antisymmetric u term, or eZ_1 term, since the difference in masses can be expressed

in terms of the difference of charges of the nuclei, so that $Z_2 = Z_1 + \Delta Z$ (see Refs. [23 and 24a]).

The coordinates of T points are practically independent of ΔZ for values in question ($\Delta Z < 0.034$). Since the Massey parameter for the u term is much greater than that for the g term, one might come to the conclusion that the cross section for such a process is much smaller than that for the opposite case $M_1 > M_2$. This is true, however, only for the direct transition via the T point. As we shall show in the next section, there exists a three-step process, realizing the reaction (1) for the asymmetric case $M_1 < M_2$ and having a cross section that is close to that for the symmetric case $M_1 = M_2$.

Figures 2(a)–2(f) show the calculated values of the rates

$$\lambda_n = \sigma_n v N \ , \tag{7}$$

reduced to the liquid-hydrogen density (LHD) $N = 4.25 \times 10^{22}$ cm^{-3}, for reactions (1) in "symmetric" and $M_1 > M_2$ cases versus collision energy ε.

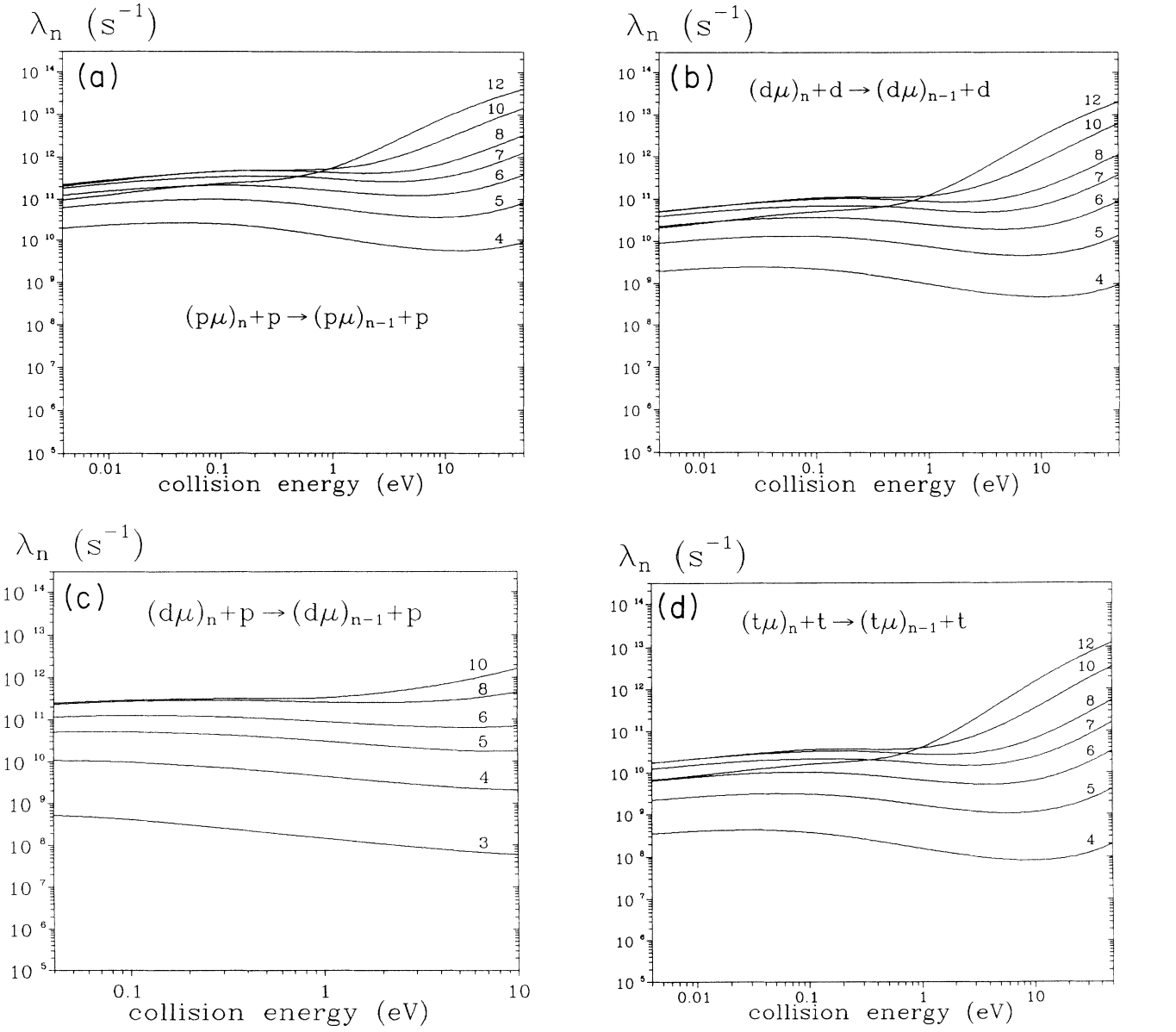

FIG. 2. (a) Rates for symmetric Coulomb deexcitation of $p\mu$ atom in collisions with hydrogen as functions of ε for different principal quantum numbers n indicated on curves. (b) Rates for symmetric Coulomb deexcitation of $d\mu$ atom in collision with deuterium as functions of ε for different n indicated on curves. (c) Rates for Coulomb deexcitation of $d\mu$ atom in collision with protium as functions of ε for different n indicated on curves. (d) Rates for symmetric Coulomb deexcitation of $t\mu$ atom in collision with tritium as functions of ε for different n indicated on curves. (e) Rates for Coulomb deexcitation of $t\mu$ atom in collision with deuterium as functions of ε for different n indicated on curves. (f) Rates for Coulomb deexcitation of $t\mu$ atom in collision with protium as functions of ε for different n indicated on curves.

TABLE V. T and P series of branch points obtained for the principal quantum number n and $\Delta = n_1 - n_2$.

		P series		T series				P series		T series	
n	$-\Delta$	ReR_c	ImR_c	ReR_c	ImR_c	n	$-\Delta$	ReR_c	ImR_c	ReR_c	ImR_c
2	1	24.8	4.1				6	340	18.7	226	40.5
							5	309	18.9	207	39.2
3	2	53.6	6.5				4	278	19.2	185.5	37.9
	1	42.1	6.6				3	247	19.5	166	36.5
							2	213	20.1	145	35
4	3	93.7	8.9	45.4	15.3		1	180	21	123.7	33.4
	2	78.5	9	36.1	14.3						
	1	63	9.2	27.1	13.2	10	9	578	23.6	406	56
							8	540	23.5	381	55
5	4	145.3	11.4	80.8	71.6		7	502	23.7	356	53.3
	3	126.3	11.5	68.7	70.5		6	464	24	329	52
	2	107	11.7	57	19.4		5	425	24.2	304	50.7
	1	86.5	12	44.8	17.9		4	385	24.7	278	49
							3	345	25.2	253	47.8
6	5	208.5	13.8	126	28		2	301	26.1	227	45.9
	4	185.8	13.9	111	27		1	258	27.6	204	44.1
	3	163	14	96.8	25.8						
	2	138.8	14.4	81.8	24.5	12	11	833	28.2	605	71
	1	114.7	14.8	67.6	22.9		10	788	28.3	574	69
							9	743	28.5	544	68
7	6	283	16.2	181	34.8		8	696	28.7	513	67
	5	257	16.3	164	33.6		7	651	29	482	65
	4	230	16.5	146.5	32.4		6	603	29.4	450	64
	3	203	16.8	128.5	31.1		5	556	29.8	420	62
	2	173	17.3	112	29.7		4	506	30.5	388	60.5
	1	144	17.6	94.2	28		3	457	31.1	357	59
							2	402	32.4	326	57.1
8	7	370	18.6	246	41.6		1	349	34.6	297	55.1

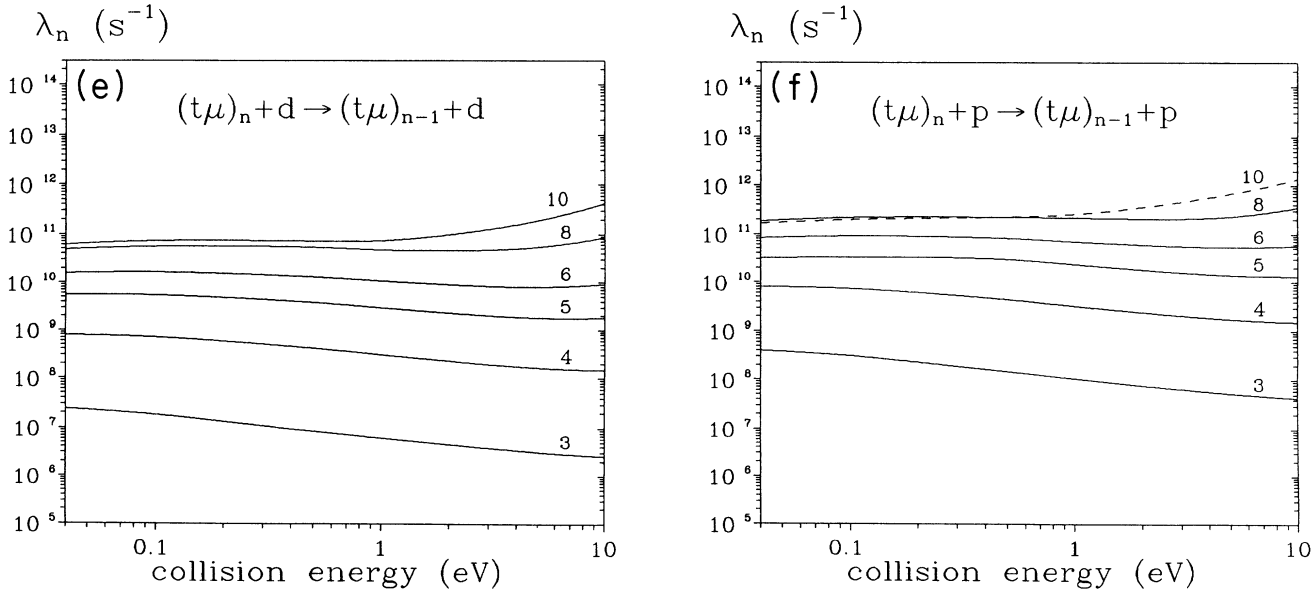

FIG. 2. (*Continued*).

III. MUON TRANSFER

A. Quasiresonant reactions

Muon transfer reactions,

$$(d\mu)_n + t \rightarrow (t\mu)_n + d \ , \tag{8}$$

$$(p\mu)_n + d \rightarrow (d\mu)_n + p \ , \tag{9}$$

$$(p\mu)_n + t \rightarrow (t\mu)_n + p \ , \tag{10}$$

represent quasiresonant reactions for which initial and final terms in the limit $R \rightarrow \infty$ differ by a small value of the resonance defect $\Delta U = (\mu_2 - \mu_1)/2n^2 = 48n^{-2}$ eV for Eq. (8), $135n^{-2}$ eV for Eq. (9), and $183n^{-2}$ eV for Eq. (10), μ_1 and μ_2 being reduced masses of the initial and final muonic atoms, respectively. For energies smaller than the resonance defect the reactions (8)–(10) are irreversible. It is clear, however, that for $\varepsilon > \Delta U$ inverse transfer reactions can proceed,

$$(t\mu)_n + d \rightarrow (d\mu)_n + t \ , \tag{11}$$

$$(d\mu)_n + p \rightarrow (p\mu)_n + d \ , \tag{12}$$

$$(t\mu)_n + p \rightarrow (p\mu)_n + t \ . \tag{13}$$

The larger the n the lower the threshold for inverse reactions (11)–(13).

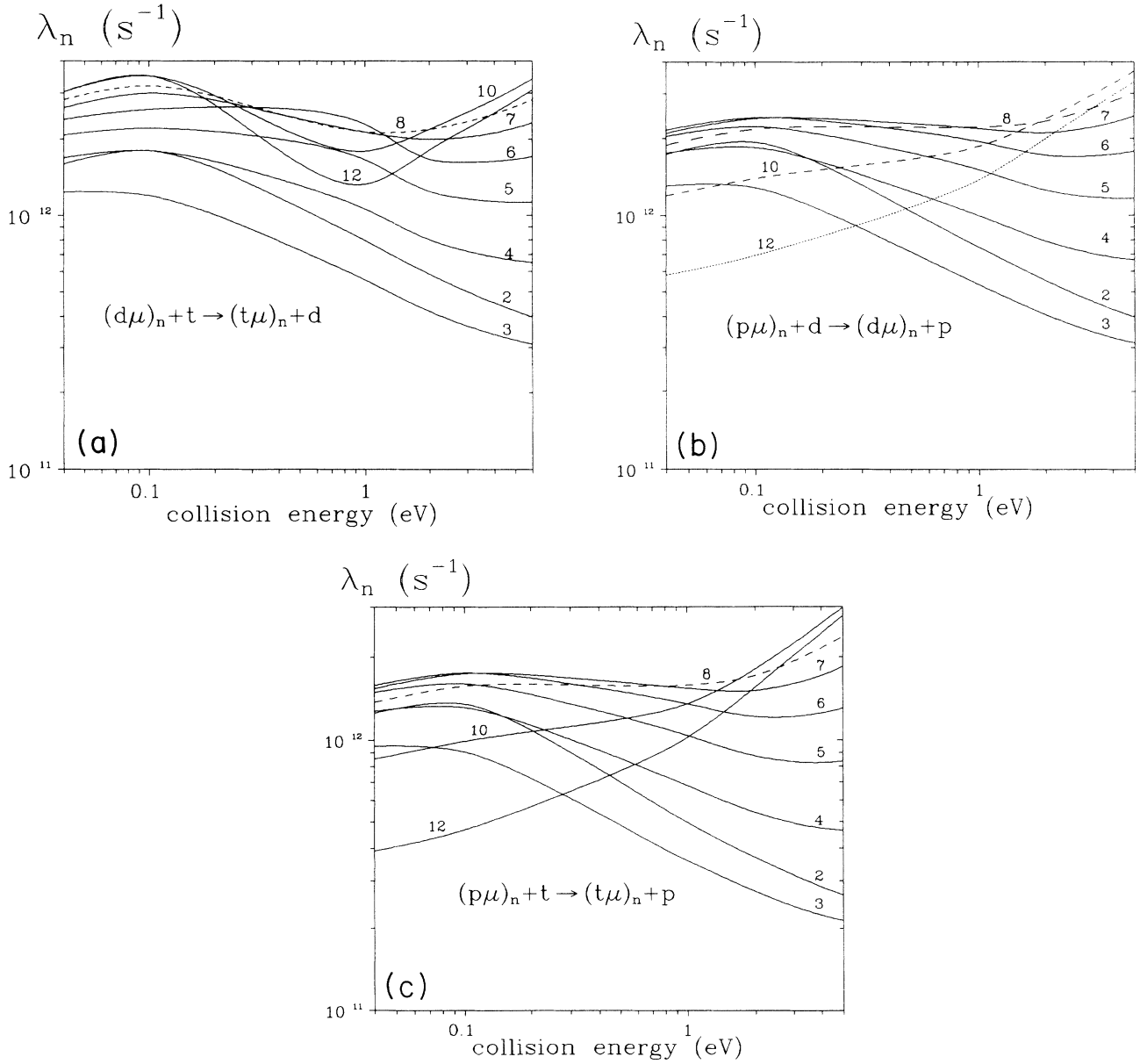

FIG. 3. (a) Rates for direct quasiresonant muon transfer from deuterium to tritium as functions of ε for different n indicated on curves. (b) Rates for direct quasiresonant muon transfer from protium to deuterium as functions of ε for different n indicated on curves. (c) Rates for direct quasiresonant muon transfer from protium to tritium as functions of ε for different n indicated on curves.

According to Ref. [23], quasiresonant reactions (8)–(13) are determined by a P series of the branch points, which arise due to exchange interactions and form an infinite family of branch points with approximately equal $\mathrm{Re}R_p$. All these points connect the given initial term (n,n_1,n_2,m) with the final one, which has the same quantum numbers but different muon localization.

The reaction probability (for double passing the transition region) is [7]

$$P=(2\cosh^2\delta)^{-1}\,, \tag{14}$$

which follows from the fact that there is an infinite family of branch points instead of a single one. Table V contains coordinates of the branch points of the P series for reactions (8) and (11). The corresponding rates for reactions (8)–(10) are demonstrated in Figs. 3(a)–3(c).

As follows from the comparison of our data for cross sections and rates of the reactions (8)–(10) with the corresponding ones of Ref. [7], new results are smaller than former ones for large n. It is explained by consideration here of the electron transfer from target nucleus to initial muonic atom nucleus during muon transfer process. The quenching factor arises from the overlap of the initial and final electron wave functions for large distances.

Figure 4(a) presents the rates as a function of principal quantum number n for reactions (8) and (11). As follows from these figures the rates of the inverse processes are very close to the rates of the direct ones. The analogous situation holds for H-D and H-T mixtures. Rates for reactions (12) and (13) are presented in Figs. 4(b) and 4(c), respectively.

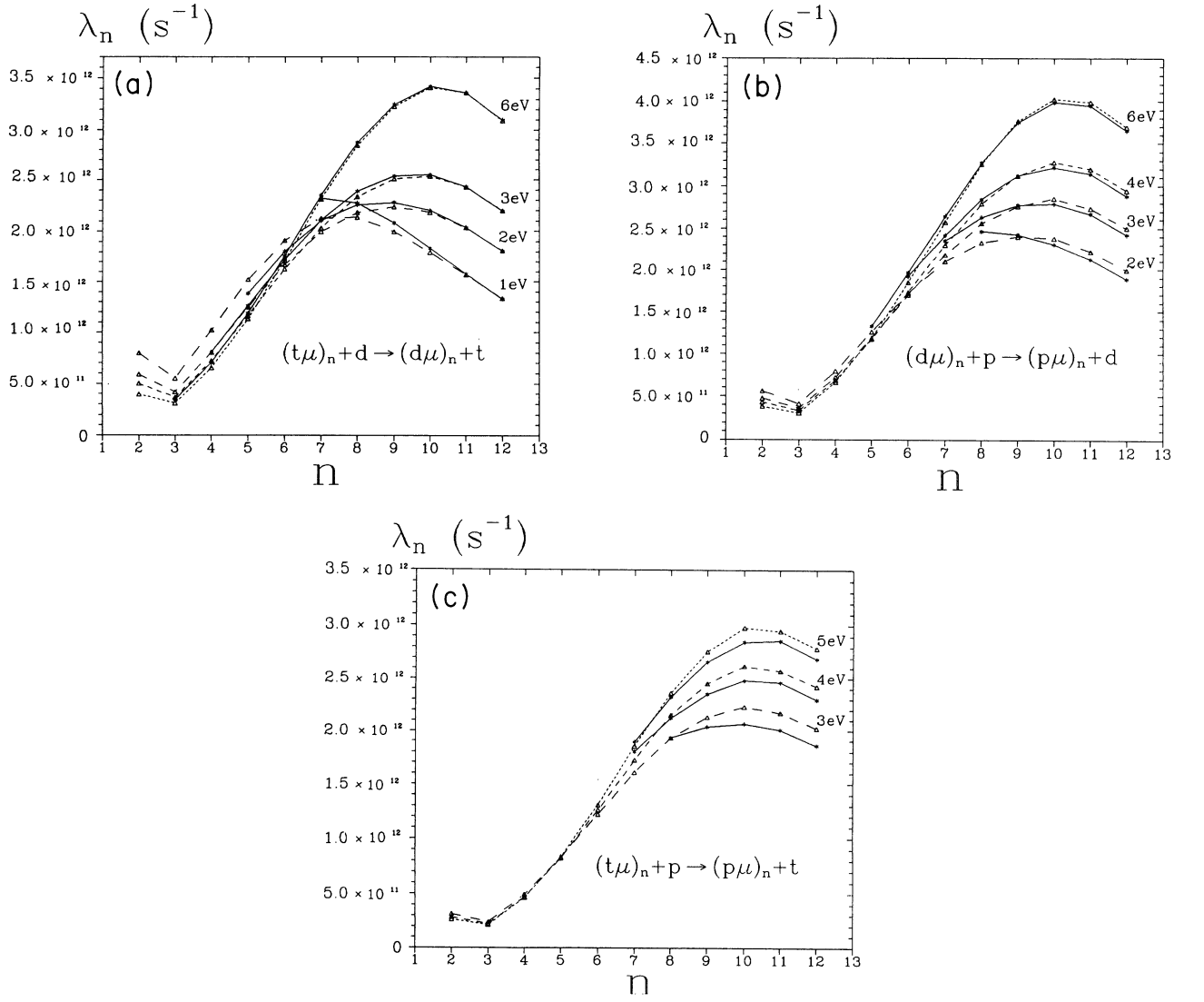

FIG. 4. (a) Rates for inverse quasiresonant muon transfer from tritium to deuterium (solid lines) as functions of n for different ε indicated on curves. The curves for direct muon transfer are also shown for comparison (dotted lines). (b) Rates for inverse quasiresonant muon transfer from deuterium to protium (solid lines) as functions of n for different ε indicated on curves. The curves for direct muon transfer are also shown for comparison (dotted lines). (c) Rates for inverse quasiresonant muon transfer from tritium to protium (solid lines) as functions of n for different ε indicated on curves. The curves for direct muon transfer are also shown for comparison (dotted lines).

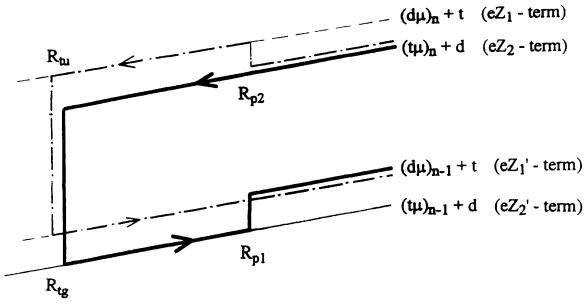

FIG. 5. Figure illustrates inverse muon transfer from tritium to deuterium as a two-step process. The notation is explained in the text.

B. Nonresonant reactions

Inverse muon transfer is possible also via reactions

$$(t\mu)_n + d \rightarrow (d\mu)_{n-1} + t \ , \tag{15}$$

$$(d\mu)_n + p \rightarrow (p\mu)_{n-1} + d \ , \tag{16}$$

$$(t\mu)_n + p \rightarrow (p\mu)_{n-1} + t \ , \tag{17}$$

which can be realized even for the lowest collision energy since the energy gain in deexcitation $\Delta U \sim (n-1/2)/n^2(n-1)^2$ is much higher than the threshold for the inverse muon transfer.

According to Ref. [23], such a process develops as a two-step process for which two ways are possible:

(a) The first transition proceeds from the initial eZ_2

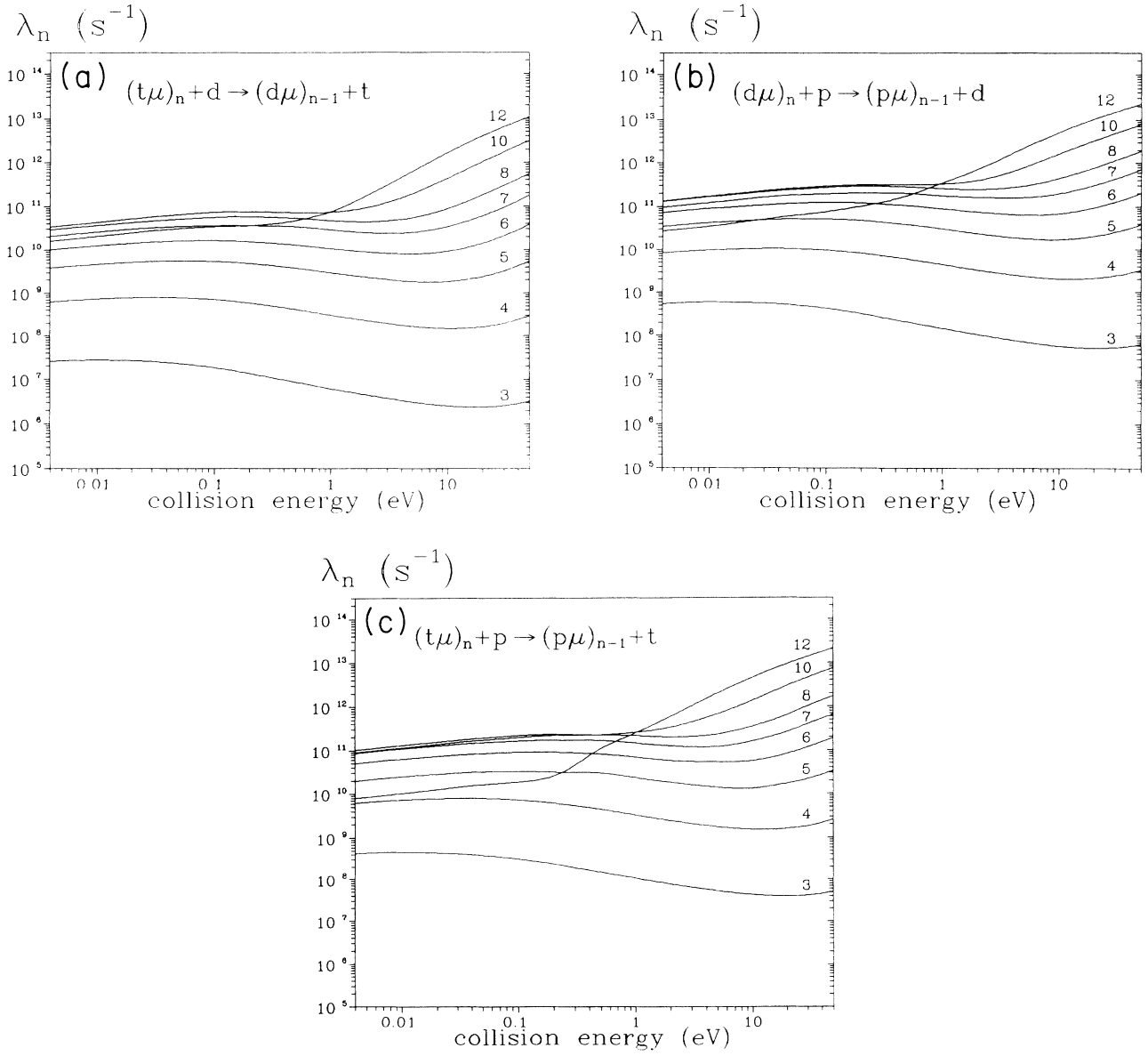

FIG. 6. (a) Rates for inverse muon transfer from tritium to deuterium as functions of ε for different n indicated on curves. (b) Rates for inverse muon transfer from deuterium to protium as functions of ε for different n indicated on curves. (c) Rates for inverse muon transfer from tritium to protium as functions of ε for different n indicated on curves.

term via the T point (g transition), then the system comes from the lower eZ_2' term to the eZ_1' one via the $p1$ point (Fig. 5). This way turns out to be the main one due to the higher probability.

(b) The first transition proceeds from the initial eZ_2 term to the eZ_1 one via the $p2$ point (there is enough energy for this reaction due to the acceleration on the way to the $p2$ point). Then transition to the lower eZ_1' term follows via the T point (u transition).

The corresponding reaction probabilities are

$$P_a = 2P_{tg}(1-P_{tg})(1-P_{p2})P_{p1} ,$$

$$P_b = 2P_{tu}(1-P_{tu})(1-P_{p1})P_{p2} ,$$

where $P_{tg}=\exp(-2\delta_{tg})$, $P_{tu}=P_{tg}^2$, $P_{pi}=(1-\tanh\delta_{pi})/2$ are the probabilities of the corresponding transitions (for single passing). The probabilities P_a and P_b are determined by the squares of the transition amplitudes, corresponding to two possible ways of the reaction. The total transition probability contains also the product of these amplitudes (interference term). It is proportional to the cosine of the energy-dependent phase difference $\Delta\alpha$, which is large in the frame of the Wentzel-Kramers-Brillouin approximation. Thus the interference term oscillates quickly [24(b)] and disappears after averaging over the small macroscopic range of acceptable momenta (and/or angles), which is necessary to compare the theory with experiment. So one can write the total transition probability as $P=P_a+P_b$.

The transfer rates for reactions (15)–(17) are given in Figs. 6(a)–6(c). The analogous two-step process is also

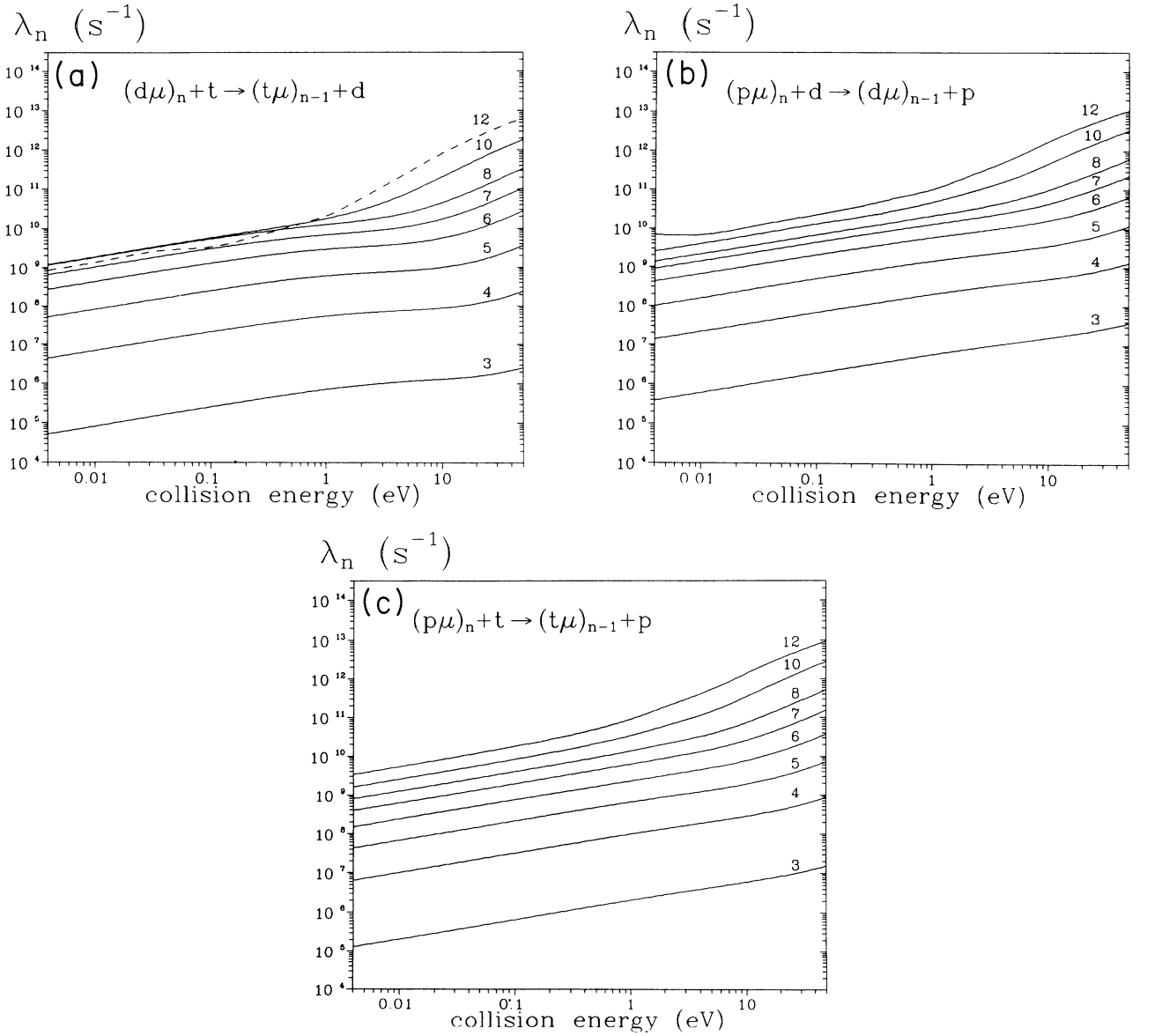

FIG. 7. (a) Rates for direct muon transfer (with decreasing n) from deuterium to tritium as functions of ε for different n indicated on curves. (b) Rates for direct muon transfer (with decreasing n) from protium to deuterium as functions of ε for different n indicated on curves. (c) Rates for direct muon transfer (with decreasing n) from protium to tritium as functions of ε for different n indicated on curves.

possible for the following direct muon transfer reactions:

$$(d\mu)_n + t \rightarrow (t\mu)_{n-1} + d \ , \tag{18}$$

$$(p\mu)_n + d \rightarrow (d\mu)_{n-1} + p \ , \tag{19}$$

$$(p\mu)_n + t \rightarrow (t\mu)_{n-1} + p \ . \tag{20}$$

The corresponding rates are presented in Figs. 7(a)–7(c), respectively. As follows now from Fig. 5, the "asymmetric" Coulomb deexcitation process, e.g., the reaction

$$(d\mu)_n + t \rightarrow (d\mu)_{n-1} + t \ , \tag{21}$$

which is suppressed as a direct process because $\mathrm{Im}R_{tu} \simeq 2\,\mathrm{Im}R_{tg}$, may be realized as a three-step process

$$(d\mu)_n + t \rightarrow (t\mu)_n + d \ , \tag{22}$$

$$(t\mu)_n + d \rightarrow (t\mu)_{n-1} + d \ , \tag{23}$$

$$(t\mu)_{n-1} + d \rightarrow (d\mu)_{n-1} + t \ , \tag{24}$$

which is realized via branch points R_{p1} for Eq. (22) and R_{p2} for Eq. (24) of the P series as well as via the "gerade" branch point R_{tg} for Eq. (23) of the T series. Two extra P transitions do not suppress the cross section due to the low values of the Massey parameter for the P transition, so $P_{pi} \simeq 1/2$.

The rates for the "asymmetric" Coulomb deexcitation are shown in Figs. 8(a)–8(c).

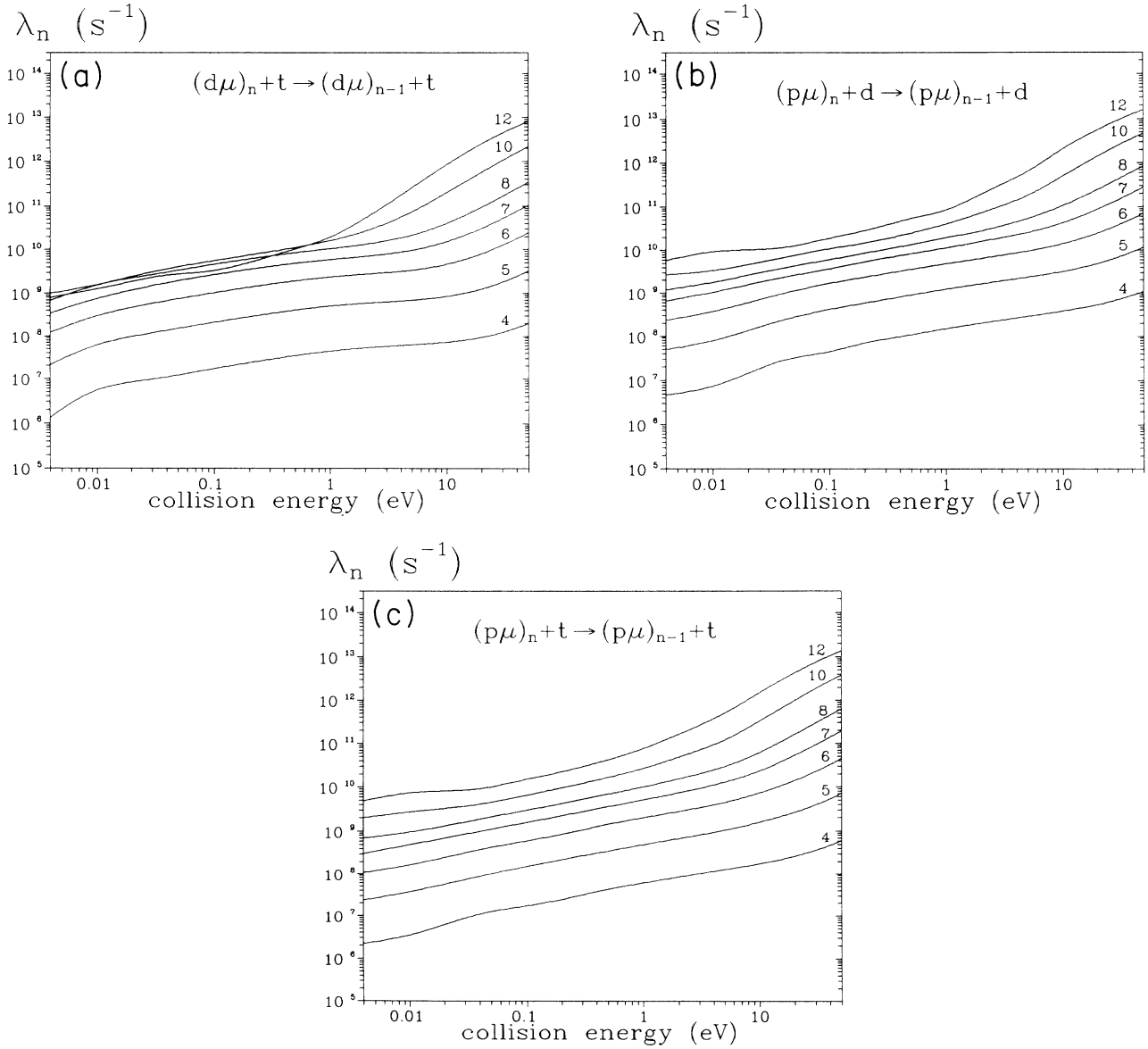

FIG. 8. (a) Rates for asymmetric Coulomb deexcitation of $d\mu$ in collision with tritium as functions of ε for different n indicated on curves. (b) Rates for asymmetric Coulomb deexcitation of $p\mu$ in collision with deuterium as function of ε for different n indicated on curves. (c) Rates for asymmetric Coulomb deexcitation of $p\mu$ in collision with tritium as function of ε for different n indicated on curves.

IV. RESULTS AND DISCUSSION

The present calculation of the q_{1s} parameter includes an inverse muon transfer in contrast with the previous ones. However, the quantum number n above which the inverse process is allowed depends on collision energy, i.e., it is allowed for ε greater than the resonant defect for a given n. The larger the n the smaller the resonance defect and, hence, the threshold for quasiresonant inverse charge exchange. In the D-T mixture for $n \sim 10$ the process can proceed above a threshold energy $\varepsilon \sim 0.5$ eV, which increases with decreasing n.

Figure 9 illustrates the energy dependence of minimal $n = \tilde{n}$, for which an inverse charge exchange is still possible.

Let us consider the influence of the inverse charge exchange on the population of the state n of muonic deuterium. Let $N(d \to t)$ and $N(t \to d)$ be the numbers of the corresponding muon transfers (in a unit of time and unit of volume). Then

$$N(d \to t) = \lambda(d \to t)\phi c_t N_{d\mu} ,$$

$$N(t \to d) = \lambda(t \to d)\phi c_d N_{t\mu} ,$$

where $N_{d\mu}$ and $N_{t\mu}$ are the densities of the $d\mu$ and $t\mu$ atoms in the state in question n. Since Coulomb capture rates of muon by deuterium and tritium are equal, the following equation is satisfied:

$$c_t N_{d\mu} = c_d N_{t\mu} . \tag{25}$$

Then the change of the number of muonic deuterium atoms, caused by the quasiresonant change exchange, is determined by the difference of the corresponding rates,

$$N(d \to t) - N(t \to d) = [\lambda(d \to t) - \lambda(t \to d)]\phi c_t N_{d\mu} .$$

While the collision energy is higher than the resonance defect, the rates of the direct and inverse charge exchange are almost equal, so these processes practically do not influence the population of the higher levels $n > \tilde{n}$

TABLE VI. Parameter q_{1s} for the D-T mixture as a function of tritium concentration c_t calculated for different densities ϕ of the mixture for $\varepsilon = 0.04$, eV (a), 2 eV (b), 3 eV (c), and 4 eV (d).

$c_t\phi$ \ (LHD)	0.1	0.5	1	1.2	$c_t\phi$ \ (LHD)	0.1	0.5	1	1.2
	(a) $\varepsilon = 0.04$ eV					(c) $\varepsilon = 3$ eV			
0.0000	1.0000	1.0000	1.0000	1.0000	0.0000	1.0000	1.0000	1.0000	1.0000
0.0010	0.9601	0.9451	0.9408	0.9398	0.0010	0.9990	0.9975	0.9967	0.9965
0.0100	0.8348	0.7766	0.7609	0.7576	0.0100	0.9899	0.9752	0.9679	0.9658
0.0200	0.7573	0.6789	0.6586	0.6546	0.0200	0.9801	0.9514	0.9375	0.9335
0.0400	0.6366	0.5378	0.5141	0.5095	0.0400	0.9611	0.9071	0.8814	0.8742
0.0600	0.5412	0.4356	0.4117	0.4072	0.0600	0.9429	0.8664	0.8308	0.8209
0.0800	0.4637	0.3582	0.3355	0.3312	0.0800	0.9255	0.8289	0.7849	0.7728
0.1000	0.3998	0.2982	0.2771	0.2732	0.1000	0.9089	0.7944	0.7433	0.7293
0.2000	0.2055	0.1354	0.1227	0.1204	0.2000	0.8354	0.6555	0.5819	0.5626
0.3000	0.1161	0.0709	0.0633	0.0619	0.3000	0.7749	0.5560	0.4726	0.4516
0.4000	0.0702	0.0406	0.0359	0.0351	0.4000	0.7244	0.4817	0.3948	0.3734
0.5000	0.0447	0.0249	0.0218	0.0213	0.5000	0.6817	0.4243	0.3370	0.3161
0.6000	0.0296	0.0160	0.0139	0.0136	0.6000	0.6452	0.3789	0.2928	0.2727
0.7000	0.0203	0.0107	0.0093	0.0090	0.7000	0.6136	0.3422	0.2581	0.2389
0.8000	0.0143	0.0074	0.0064	0.0062	0.8000	0.5862	0.3120	0.2303	0.2120
0.9000	0.0104	0.0052	0.0045	0.0044	0.9000	0.5621	0.2869	0.2077	0.1902
1.0000	0.0076	0.0038	0.0033	0.0032	1.0000	0.5410	0.2656	0.1890	0.1723
	(b) $\varepsilon = 2$ eV					(d) $\varepsilon = 4$ eV			
0.0000	1.0000	1.0000	1.0000	1.0000	0.0000	1.0000	1.0000	1.0000	1.0000
0.0010	0.9976	0.9958	0.9949	0.9946	0.0010	0.9990	0.9976	0.9969	0.9968
0.0100	0.9760	0.9589	0.9506	0.9482	0.0100	0.9906	0.9769	0.9702	0.9683
0.0200	0.9530	0.9202	0.9046	0.9002	0.0200	0.9813	0.9548	0.9420	0.9383
0.0400	0.9092	0.8495	0.8217	0.8140	0.0400	0.9634	0.9132	0.8895	0.8828
0.0600	0.8685	0.7866	0.7494	0.7391	0.0600	0.9463	0.8748	0.8418	0.8326
0.0800	0.8304	0.7302	0.6858	0.6736	0.0800	0.9298	0.8394	0.7983	0.7870
0.1000	0.7949	0.6796	0.6296	0.6161	0.1000	0.9140	0.8065	0.7585	0.7454
0.2000	0.6477	0.4899	0.4281	0.4121	0.2000	0.8436	0.6724	0.6020	0.5835
0.3000	0.5386	0.3687	0.3072	0.2920	0.3000	0.7849	0.5746	0.4938	0.4732
0.4000	0.4554	0.2866	0.2297	0.2160	0.4000	0.7353	0.5005	0.4153	0.3942
0.5000	0.3904	0.2287	0.1773	0.1653	0.5000	0.6929	0.4425	0.3563	0.3354
0.6000	0.3388	0.1864	0.1404	0.1299	0.6000	0.6562	0.3962	0.3105	0.2903
0.7000	0.2971	0.1546	0.1136	0.1044	0.7000	0.6242	0.3583	0.2743	0.2549
0.8000	0.2629	0.1302	0.0936	0.0855	0.8000	0.5961	0.3270	0.2451	0.2265
0.9000	0.2344	0.1111	0.0783	0.0712	0.9000	0.5712	0.3006	0.2211	0.2033
1.0000	0.2106	0.0958	0.0663	0.0601	1.0000	0.5490	0.2782	0.2010	0.1841

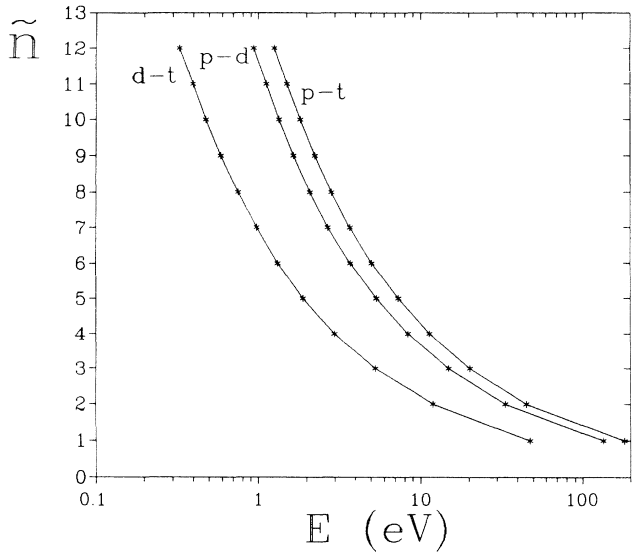

FIG. 9. Energy dependence of minimal principal quantum number $\tilde{n}$ for which the inverse quasiresonant muon transfer is possible.

and may be neglected in principle. For $n \leq \tilde{n}$ the resonance defect is higher than the collision energy and inverse charge exchange is forbidden, which makes the relation (25) invalid. For this reason the processes of the inverse charge exchange with the deexcitation begin to influence the population of the lower states. At the same time, for lower states the rates of such processes are small compared with those of radiative and Auger deexcitations as well as quasiresonant direct charge exchange. However, all deexcitation and transfer processes, indicated in Fig. 1, are taken into account in our calculations of q_{1s}.

The q_{1s} values were obtained by solving the system of kinetic equations with the initial conditions corresponding to the populations $q_{12}=1$ and $q_{i<12}=0$. The data for q_{1s} as a function of the concentration of heavier hydrogen isotope c_i and density ϕ in LHD units are shown, for the D-T mixture, in Tables VI. Such dependence of q_{1s} for all mixtures of hydrogen isotopes is presented in Figs.

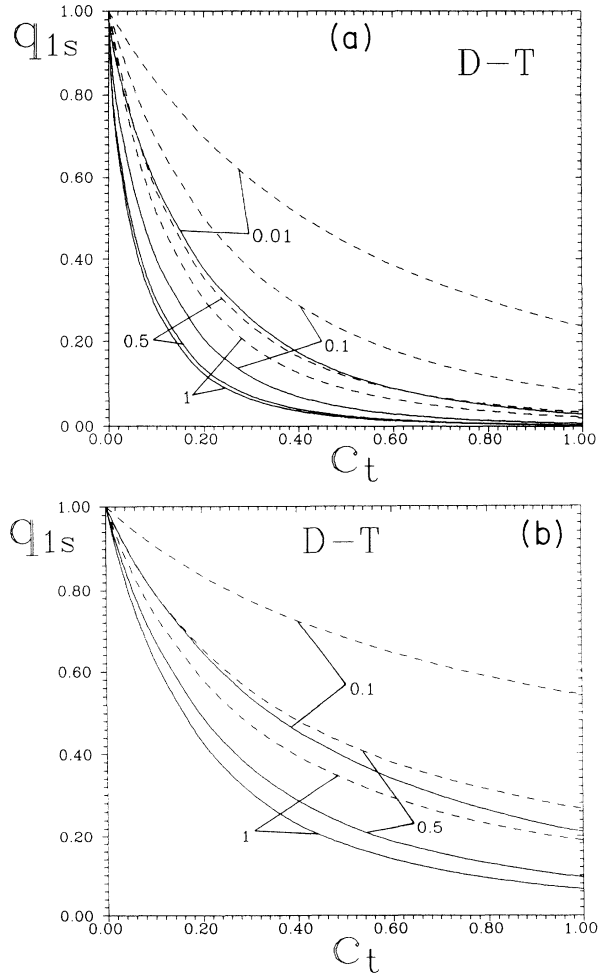

FIG. 10. (a) Parameter q_{1s} for D-T mixture as function of tritium concentration c_t calculated for $\varepsilon=0.04$ (solid lines) and 1 eV (dashed lines) and different target densities (in LHD units), indicated on the curves. (b) Parameter q_{1s} for D-T mixture as a function of tritium concentration c_t calculated for $\varepsilon=2$ (solid lines) and 3 eV (dashed lines) and different target densities (in LHD units), indicated on the curves.

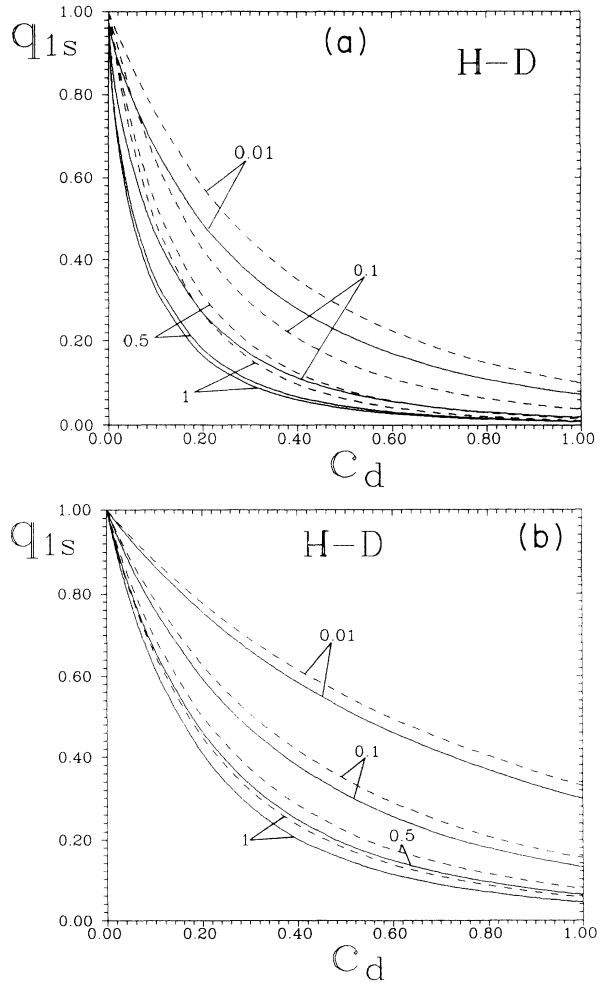

FIG. 11. (a) Parameter q_{1s} for the H-D mixture as a function of deuterium concentration c_d calculated for $\varepsilon=0.04$ (solid lines) and 1 eV (dashed lines) and different target densities (in LHD units), indicated on the curves. (b) Parameter q_{1s} for the H-D mixture as a function of deuterium concentration c_d calculated for 2 (solid lines) and 3 eV (dashed lines) and different target densities (in LHD units), indicated in the curves.

10–12 for different ϕ and ε.

As follows from the comparison of experimental data [8] and our q_{1s} results [see Figs. 13(a) and 13(b)] the collision energy of excited muonic deuterium in the D-T mixture stay within a range $2<\varepsilon\leq 3$ eV which corresponds to $\bar{n}=4$. Thus, the decisive stage of the cascade begins from $n=4$ where the electron screening and molecular binding effects, as well as the above mentioned effect of electron transfer, are not as important as for highly excited muonic hydrogen. Therefore, the results obtained are reliable enough. Nevertheless, the role of electron screening for higher states is very important both for direct (see Ref. [7]) and inverse muon transfer.

Our conclusion about the high collision energy of the excited muonic deuterium is in agreement with some other available experimental data [25], where fast muonic atoms (with the kinetic energies from several eV to several tens of eV) in the ground state have been observed. High collision energy of excited muonic hydrogen could be explained by small elastic cross sections (which are responsible for the deceleration of excited muonic atoms by elastic collisions) owing to the Ramsauer-Townsend effect, which cannot be excluded. An alternative explanation could be owing to possible acceleration of muonic hydrogen during cascade deexcitation (e.g., because of the Coulomb deexcitation). So far, however, both experimental and theoretical data on elastic cross sections for excited muonic hydrogen are still absent. As for the H-D mixture, the preliminary experimental data on q_{1s} (obtained for $c_d=0.2$ and LHD) are compared with our calculations in Fig. 14. In fact, the resonance defect in the H-D mixture is larger than in the D-T one, so for $\varepsilon\sim 3$ eV, $\bar{n}=7$, which leads to somewhat lower q_{1s} values. At the same time, the experimental re-

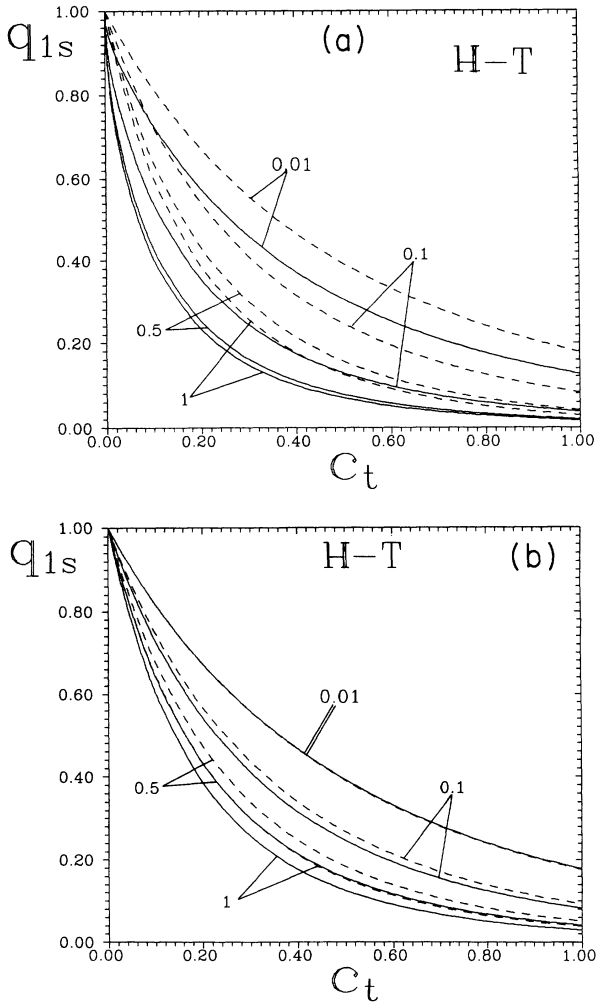

FIG. 12. (a) Parameter q_{1s} for the H-T mixture as a function of tritium concentration c_t calculated for $\varepsilon=0.04$ (solid lines) and 1 eV (dashed lines) and different target densities (in LHD units), indicated on the curves. (b) Parameter q_{1s} for the H-T mixture as a function of tritium concentration c_t calculated for $\varepsilon=1$ (solid lines) and 2 eV (dashed lines) and different target densities (in LHD units), indicated in the curves.

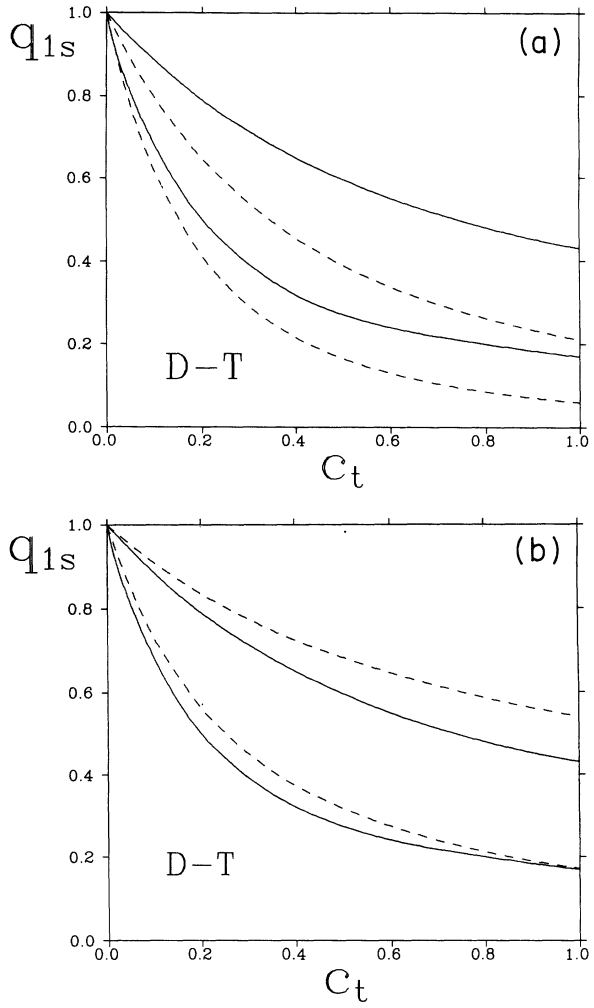

FIG. 13. (a) Comparison of experimental data on q_{1s} [8] (solid lines) for the D-T mixture with the theoretical ones (dashed line), calculated for $\phi=0.1$ (upper curve) and 1.2 (lower curve) LHD and $\varepsilon=2$ eV. As follows from such comparison experimental corridor owing to error bounds practically hides the density dependence predicted theoretically. (b) Comparison of experimental q_{1s} with theoretical ones calculated for $\varepsilon=3$ eV. The notations are the same as in (a).

sult can be explained assuming collision energy $5 < \varepsilon < 6$ eV, which corresponds to $\bar{n} = 5$ and 4, respectively. According to our calculations, Coulomb deexcitation has a weak influence on q_{1s}. This process, however, may be of importance as a source of the acceleration of muonic protium. One should note that Coulomb deexcitation cross section for the H-D system is much higher than for the D-T one [see Figs. 8(a) and 8(b)], which may lead to higher collision energies for the former system. At the same time, further experimental investigation of q_{1s} in the H-D mixture is necessary.

In conclusion, we would like to underline that muon transfer from muonic hydrogen to helium nuclei is irreversible due to Coulomb repulsion between the muonic helium ion and hydrogen nucleus. Available experimental data [26,27] are in agreement with our calculations for deuterium-helium mixture [28].

Note added in proof. After this paper had been accepted for publication, new data on q_{1s} for the H-D mixture became available [P. Ackerbauer *et al.*, PSI Nucl. Part. Phys. Newsl. 53 (1993)]. The new data agree with our calculations for $\varepsilon \simeq 6$ eV, in accordance with our conclusions.

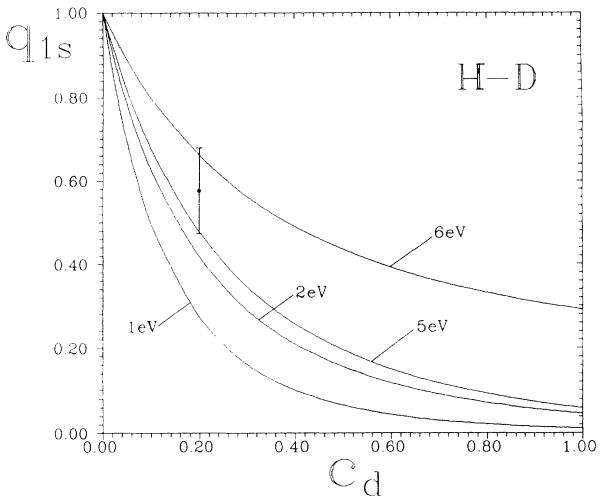

FIG. 14. Comparison of experimental q_{1s} point for H-D mixture [9] normalized to LHD with theoretical curves calculated for ε, indicated on curves.

ACKNOWLEDGMENTS

We would like to thank A. Vitale and A. Bertin for valuable discussions. We are also grateful to S. Yu. Ovchinnikov and D. I. Abramov for cooperation in calculation of branch points of the T series and quasiclassical eigenvalues of the two-center problem. One of us (N.P.) expresses his gratitude to O. J. Stadler and W. von Hoersten for support of this work. This work was financially supported by Grant No. 224109102 of the Polish Committee of Scientific Researches (KBN) on the part of the Polish co-authors.

[1] E. Fermi and E. Teller, Phys. Rev. **72**, 399 (1947).
[2] J. S. Cohen, R. J. Martin, and W. R. Wadt, Phys. Rev. A **24**, 33 (1981); *ibid.* **27**, 1821 (1983).
[3] J. S. Cohen, Phys. Rev. A **27**, 167 (1983).
[4] J. D. Garcia, N. H. Kwong, and J. S. Cohen, Phys. Rev. A **35**, 4068 (1987).
[5] H. Schneuwly, in Joint Institute for Nuclear Research Report No. JINR-D14-87-799, 1987 (unpublished), p. 347.
[6] G. Ya. Korenman and V. P. Popov, in *Muon-Catalyzed Fusion,* Proceedings of the Conference on Muon-Catalyzed Fusion, Sanibel Island, 1988, edited by S. E. Jones, J. Rafelski, and H. Monkhorst, AIP Conf. Proc. No. 181 (AIP, New York, 1989), p. 145; V. V. Balashov *et al.*, Muon Catal. Fusion **2**, 105 (1988); G. Ya. Korenman, S. V. Leonova, V. P. Popov, and V. K. Dolinov, in *Proceedings of an International Symposium on Muon Catalyzed Fusion μCF-89,* edited by J. D. Davies (Rutherford Appleton Laboratory, Chilton Didcot Oxon, UK, 1990), p. 52.
[7] W. Czapliński, A. Gula, A. Kravtsov, A. Mikhailov, and N. Popov, preceding paper, Phys. Rev. A **50**, 518 (1994), and reference therein.
[8] P. Ackerbauer *et al.*, in *Proceedings of International Workshop on LEMS'93,* edited by M. Leon, Los Alamos Laboratory Report No. LA-12698-C, 1984 (unpublished), p. 285.
[9] B. Lauss *et al.*, in *Proceedings of International Workshop on LEMS'93* (Ref. 8), p. 300.
[10] M. Leon and H. A. Bethe, Phys. Rev. **127**, 636 (1962).
[11] A. P. Bukhvostov and N. P. Popov, Zh. Eksp. Teor. Fiz. **82**, 23 (1982) [Sov. Phys. JETP **55**, 13 (1982)].
[12] H. A. Bethe and E. E. Salpeter, *Quantum Mechanics of One- and Two-Electron Atoms* (Academic, New York, 1957); M. Jandel, S. E. Jones, B. Muller, and J. Rafelski, CERN Report No. CERN-TH4856/87 (unpublished).
[13] G. Kodoski and M. Leon, Nuovo Cimento B **1**, 41 (1971).
[14] R. O. Mueller, V. W. Hughes, H. Rosental, and C. S. Wu, Phys. Rev. A **11**, 1175 (1975).
[15] G. Carboni and G. Fiorentini, Nuovo Cimento B **39**, 281 (1977).
[16] J. S. Cohen and J. N. Bardsley, Phys. Rev. A **23**, 46 (1981).
[17] L. I. Menshikov and L. I. Ponomarev, Z. Phys. D **2**, 1 (1986).
[18] A. V. Kravtsov, A. I. Mikhailov, and N. P. Popov, Phys. Lett. **A132**, 124 (1988).
[19] L. Bracci and G. Fiorentini, Nuovo Cimento **43**, 9 (1978).
[20] L. I. Menshikov, Muon Catal. Fusion **2**, 173 (1988).
[21] W. Czaplinski, A. Gula, A. Kravtsov, A. Mikhailov, S. Ovchinnikov, and N. Popov, Muon Catal. Fusion **5/6**, 59 (1990/91).
[22] W. Czaplinski, A. Gula, A. Kravtsov, A. Mikhailov, S. Ovchinnikov, and N. Popov, in *Exotic Atoms in Condensed Matter,* edited by G. Benedek and H. Schneuwly (Springer-Verlag, Berlin, 1992), p. 159.
[23] T. P. Grozdanov and E. A. Solov'ev, Phys. Rev. A **42**, 2703 (1990); E. A. Solov'ev, Usp. Fiz. Nauk **157**, 437 (1989) [Sov. Phys. Usp. **32**, 228 (1989)].
[24] (a) D. I. Abramov, S. Yu. Ovchinnikov, and E. A. Solov'ev, Phys. Rev. A **42**, 6366 (1990); (b) E. E. Nikitin and S. Ya. Umanskii, *Theory of Slow Atomic Collision* (Springer-Verlag, Berlin, 1984).
[25] G. M. Marshall *et al.*, Hyperfine Interact. **82**, 529 (1993);

F. Kottmann, in *Muonic Atoms and Molecules,* edited by L. Schaller and C. Petitjean (Burkhauser Verlag, Basel, 1993), p. 219; J. F. Crawford *et al.*, Phys. Rev. D **43**, 46 (1991).

[26] A. Bertin, A. Vitale, and E. Zavattini, Lett. Nuovo Cimento **18**, 381 (1977); A. Bertin *et al.*, in *Muon-Catalyzed Fusion* (Ref. [6]), p. 161.

[27] D. V. Balin *et al.*, in *Muonic Atoms and Molecules* (Ref. [25]), p. 25.

[28] A. Gula, A. Kravtsov, and N. Popov, in *Proceedings of an International Symposium on Muon Catalyzed Fusion* $\mu CF-89$ (Ref. [6]), p. 54.